

Genomic analysis of *Salmonella* bacteriophages revealed multiple endolysin ORFs and importance of ligand-binding site of receptor-binding protein

Mustafa Guzel^{1,2}, Aysenur Yucefaydali³, Segah Yetiskin³, Aysu Deniz³, Osman Yaşar Tel⁴, Mustafa Akçelik⁵, Yeşim Soyer^{1,3,*}

¹Department of Biotechnology, Middle East Technical University, Ankara 06800, Türkiye

²Department of Food Engineering, Hitit University, Corum 19030, Türkiye

³Department of Food Engineering, Faculty of Engineering, Middle East Technical University, Ankara 06800, Türkiye

⁴Faculty of Veterinary Medicine, Harran University, Şanlıurfa 63300, Türkiye

⁵Department of Biology, Ankara University, Ankara 06100, Türkiye

*Corresponding author. Department of Food Engineering, Faculty of Engineering, Middle East Technical University (METU) Çankaya, Ankara 06800, Türkiye. E-mail: ysoyer@metu.edu.tr

Editor: [Ville-Petri Friman]

Abstract

Salmonella is a prevalent foodborne pathogen causing millions of global cases annually. Antimicrobial resistance is a growing public health concern, leading to search for alternatives like bacteriophages. A total of 97 bacteriophages, isolated from cattle farms ($n = 48$), poultry farms ($n = 37$), and wastewater ($n = 5$) samples in Türkiye, were subjected to host-range analysis using 36 *Salmonella* isolates with 18 different serotypes. The broadest host range belonged to an Infantis phage (MET P1-091), lysing 28 hosts. A total of 10 phages with the widest host range underwent further analysis, revealing seven unique genomes (32–243 kb), including a jumpophage (>200 kb). Except for one with lysogenic properties, none of them harbored virulence or antibiotic resistance genes, making them potential *Salmonella* reducers in different environments. Examining open reading frames (ORFs) of endolysin enzymes revealed surprising findings: five of seven unique genomes contained multiple endolysin ORFs. Despite sharing same endolysin sequences, phages exhibited significant differences in host range. Detailed analysis unveiled diverse receptor-binding protein sequences, with similar structures but distinct ligand-binding sites. These findings emphasize the importance of ligand-binding sites of receptor-binding proteins. Additionally, bacterial reduction curve and virulence index revealed that Enteritidis phages inhibit bacterial growth even at low concentrations, unlike Infantis and Kentucky phages.

Keywords: antibiotic resistance; bacteriophages; biopreservation; endolysin; ligand-binding site; *Salmonella*

Introduction

Salmonella enterica subsp. enterica (*Salmonella*) is one of the four major causes of diarrhea globally (WHO 2018). The emergence of multidrug-resistant (MDR) *Salmonella* strains have become a major public health concern as it limits treatment options for infected individuals (EFSA 2022). Antimicrobial resistance is one of the most important topics in the One Health approach, which focuses on the global health threats in animal–human–environmental interface (Velazquez-Meza et al. 2022). According to the World Health Organization, unless conditions change dramatically, antibiotic-resistant bacteria are estimated to kill 10 million people globally by 2050 (de Kraker et al. 2016).

The use of bacteriophages has become popular in recent years as a promising alternative to antibiotics for the treatment of bacterial infections, including MDR *Salmonella* infections. (Carvalho et al. 2017). Bacteriophages, shortly phages, are viruses that infect bacterial cells and are the most abundant entities in nature (Puxty and Millard 2023). Phages mainly follow two different life cycles, lytic and lysogenic. The lytic cycle, also known as the virulent life cycle, including bacteriophages proliferation and destruction of their host cells, when they enter the cell (Drulis-Kawa et al. 2012), while the lysogenic cycle is characterized by the inte-

gration of the bacteriophage's genetic material into the host cell's genome. The use of obligatory virulent phages has potential applications against bacterial contamination in the One Health approach (Matsuzaki et al. 2005). Furthermore, the main mechanism of host lysis by phages is depending on their endolysin enzymes that lyse host cells by targeting the peptidoglycan (PG) layer, a highly conserved and highly invariant component of the bacterial cell wall at the end of the lytic cycle to release newly assembled phages.

Bacteriophage therapy is considered as a natural and promising method compared to antibiotics and other conventional methods, since bacteriophages offer several advantages over antibiotics. Phages solely infect target bacteria and no other microorganisms in the environment (Domingo-Calap and Delgado-Martínez 2018), therefore they do not put pressure on other bacteria to acquire resistance (Principi et al. 2019). Besides these advantages, the success of phage therapy depends on the characterization and selection of appropriate phages. First, phage efficacy against the target strains is a key characterization (Vikram et al. 2020). In addition, genetic characteristics of the phage are critical. Phages should not encode antimicrobial genes, virulence genes, or lysogenic lifestyle genes (Lavilla et al. 2023).

Received 29 February 2024; revised 2 May 2024; accepted 29 May 2024

© The Author(s) 2024. Published by Oxford University Press on behalf of FEMS. This is an Open Access article distributed under the terms of the Creative Commons Attribution Non-Commercial License (<https://creativecommons.org/licenses/by-nc/4.0/>), which permits non-commercial re-use, distribution, and reproduction in any medium, provided the original work is properly cited. For commercial re-use, please contact journals.permissions@oup.com

For commercial distribution and usage against common foodborne pathogens, the phage including products should be reviewed and cleared by legislation and be approved by local authorities, such as the Food and Drug Administration (FDA) (Vikram et al. 2020). There are several FDA-approved commercial phage-based biocontrol agent that targets *Salmonella*, including but not limited to SalmoFresh™ by Intralytix (USA), PhageGuard-S by PhageGuard (the Netherlands), Armament by Omnilytics (USA), and Biotector by Cheiljedang (South Korea). However, due to the nature of phages, these products were prepared for specific serotypes, and may not affect others. As it is known, pathogenic strains of *Salmonella* have geographically cluster in the different locations worldwide, even they share the same serotype, they might not be affected by the same type of phages. As a result, current commercial products from different countries may not be effective. It is crucial that for a successful phage product, first most prevalent and most infectious serotype strains in that region must be determined, and a target-based product should be developed.

The aim of this study was to isolate bacteriophages that infect *Salmonella* spp. Samples collected in different seasons from poultry, cattle farms, and wastewater facilities in Türkiye were used to characterize the phages for further applications using phenotypic (host range, latent period, burst size, and adsorption constant), and genotypic methods (whole genome sequencing and bioinformatic analysis). In addition, we also aimed to shed light on the infection mechanisms of these phages by using different bioinformatics tools. Also, to observe the inhibitory effects of bacteriophages on bacteria, planktonic killing assay was performed, and virulence indices were determined.

Materials and methods

Bacterial strains

To isolate phages, eight different *S. enterica* subsp. *enterica* (*Salmonella*) representing the commonly seen eight different serotypes were used (Table 1). These isolates were collected from various sources in Türkiye and stored at -80°C at the Food Engineering Department, Middle East Technical University (METU). All strains were inoculated into 10 ml of Luria–Bertani (LB) broth for phage isolation and incubated at 37°C for 18–20 h.

To determine the host range of phages, a wider set of *Salmonella* isolates ($n = 36$) representing 18 different serotypes that were the most common and rare serotypes in general and collected from different studies in Türkiye, were used (Acar et al. 2017). These isolates were selected based on their source, antimicrobial resistance profiles, and molecular subtypes [pulsed-field gel electrophoresis (PFGE) subtype] (Table 1). Also, MET S1-015 (*S. Montevideo*) is used for both phage isolation and host range determination.

Sampling

A total of 85 samples were collected from cattle ($n = 48$) and poultry ($n = 37$) farms from different regions of Türkiye, including the Southeastern Anatolia, Central Anatolia, Black Sea, and Marmara regions, in every season from 2020 to 2021 (Supplementary Table 1). In addition, five samples were collected at the METU wastewater facility in Ankara.

Bacteriophage isolation and double plaque assay

In total, 10 g of stool samples from farms were mixed with 100 ml salt magnesium (SM) buffer, then incubated at 37°C for 2 h in a shaking incubator and centrifuged at $9000 \times g$ for 10 min and fil-

tered through $0.22 \mu\text{m}$ filter. *Salmonella* Enteritidis (MET S1-001), Typhimurium (MET S1-002), and Infantis (MET S1-006), isolates (Table 1) were used as hosts for the samples. A volume of 5 ml of sample was pre-enriched with 100 μl of each strain and 5 ml of 2x tryptic soy broth. After overnight incubation at 37°C , the samples were centrifuged and filtered to obtain a phage solution that was stored at 4°C (Huang et al. 2018). Samples from the wastewater were processed in the same manner, but with an additional five *Salmonella* isolates (MET S1-248, MET S1-015, MET S1-063, MET S1-007, and MET S1-163), representing five serotypes; Anatum, Montevideo, Telaviv, Kentucky, and Hadar (Table 1). Phage presence was assessed using a double-plaque assay. The phage solution and host (100 μl) were added to 4 ml of 0.6% LB agar, mixed, and poured onto solid LB agar. Plaques were observed after overnight incubation at 37°C .

Bacteriophage purification and titer determination

Morphologically different phage plaques were detected using a double plaque assay. Each plaque that appeared morphologically different was purified. Selected plaques with different morphologies were transferred to 100 μl of 0.9% NaCl solution and placed in an Eppendorf tube using a sterile pipette tip. Serial dilutions of up to 10^{-8} were prepared, and double plaque assays were made from 10^{-3} to 10^{-8} dilutions. The purification step was performed at least three times until a uniform morphology was observed. After the uniform morphology was observed, saline magnesium (SM) buffer (1 M Tris-HCl pH: 7.5, 0.1 M NaCl, 0.01 M $\text{MgSO}_4 \cdot 7\text{H}_2\text{O}$, and 2% gelatin) was added to a Petri dish to collect the plaques. After waiting for 30 min at room temperature, the buffer was collected and centrifuged at $9000 \times g$ for 10 min and filtered through $0.22 \mu\text{m}$ filter. Each filtered lysate was stored under a different METU ID at 4°C and -80°C at the Food Engineering Department, Middle East Technical University.

Host-range determination

Host-range analysis was conducted to determine the spectrum of bacterial strains that a particular bacteriophage can infect and replicate within. A total of 36 isolates representing 18 different serotypes were used to determine the host range (Table 1). *Salmonella enterica* ssp. *enterica* includes the main serotypes causing infections in warm-blooded animals, so this study did not focus on *Salmonella bongori* and other *S. enterica* ssp. that infect humans rarely. The phages isolated in our study were tested against the same species of *Salmonella* (*S. enterica* ssp. *enterica*), but multiple strains representing common and rare serotypes (Typhimurium, Enteritidis, Infantis, Anatum, Telaviv, Montevideo, Hadar, Kentucky, Paratyphi, and so on). For the most frequent serotypes, multiple isolates were selected from various sources with different PFGE types. The host range was determined according to modified protocols (Fong et al. 2017, Moreno Switt et al. 2013). Host cells (100 μl) were added to semisolid (0.6% agar) LB agar and poured onto solid LB plates with gentle mixing. After solidification, the Petri dish was divided into eight pieces and labeled. A volume of 5 μl of the corresponding phage were spotted on each fragment. The samples were left to dry at room temperature and incubated overnight at 37°C . One day later, the formations on the Petri dish were examined, and the spots were graded according to the cleanliness of the zone. Ten phages with the broadest host range that can infect the most common serotypes were selected for further characterization.

Table 1. *Salmonella* isolates that are used as target strains in phage isolation and host range.

METUID	Serogroup	Serotype	Isolate source	Antibiotic resistance**	PFGE type***
MET S1-001	D1	Enteritidis	Chicken meat	Susceptible	NA
MET S1-742	D	Enteritidis	Food	Susceptible	PT06
MET S1-217	D	Enteritidis	Human	Susceptible	PT04
MET S1-221	D	Enteritidis	Human	Susceptible	PT05
MET S1-411	D	Enteritidis	Food	Susceptible	PT51
MET A2-012	D	Enteritidis	Sludge	Susceptible	PT55
MET S1-002	B	Typhimurium	Chicken meat	CipAzm	NA
MET S1-223	B	Typhimurium	Human	TAm	PT23
MET S1-185	B	Typhimurium	Human	Sf	PT15
MET S1-663	B	Typhimurium	Animal (sheep)	TAmKf	PT13
MET A2-003	B	Typhimurium	Sludge	Susceptible	PT59
MET A2-088	B	Typhimurium	DT104	NI	NI
MET S1-657	B	Typhimurium	Animal (sheep)	STAmAmsfCn	PT14
MET S1-006	C1	Infantis	Chicken meat	KKfSxtSfNCip	NA
MET S1-050	C1	Infantis	Food	KSTAmSfN	PT08
MET S1-807	C1	Infantis	Human	CroEftSfSxtCKSAmp AmcTeFoxKf	NI
MET S1-857	C1	Infantis	Sludge	Susceptible	PT73
MET S1-007	C3	Kentucky	Chicken meat	Susceptible	NA
MET S1-240	C3	Kentucky	Human	Susceptible	PT10
MET S1-542	C3	Kentucky	Animal (sheep)	Sf	PT03
MET A2-072	C3	Kentucky	Sludge	KfSfAmpNAzmPef	PT72
MET S1- 015	C1	Montevideo	Ground meat	KSTSfN	NA
MET S1-065	C1	Montevideo	Food	SfSxtNT	PT25
MET S1-170	C1	Montevideo	Animal (cattle)	Susceptible	PT44
MET S1-172	C1	Montevideo	Animal (cattle)	Sf	PT31
MET S1-248	E1	Anatum	Sheep ground meat	Susceptible	PT42
MET S1-548	E	Anatum	Food	Susceptible	PT42
MET S1-579	E	Anatum	Food	Susceptible	PT42
MET S1-163	C2	Hadar	Food	AmpKfN	PT41
MET S1-063	M	Telaviv	Offal	Susceptible	PT33
MET S1-074	M	Telaviv	Food	SfSxtNT	PT33
MET S1-530	M	Telaviv	Food	Susceptible	PT34
MET S1-008	C	Thompson	Food	KSTAmKfSfSxtCn	NA
MET S1-010	E	Senftenberg	Food	STSFN	NA
MET S1-087	E	Othmarschen	Food	Susceptible	PT27
MET S1-166	C2	Newport	Animal (cattle)	Sf	PT39
MET S1-713	C1	Braenderup	NI	NI	PFGE Ref.
MET S1-864	C1	Mbandaka	Sludge	SxtSfAmpAzmPef	PT65
MET A2-099	E	Liverpool	Food	Susceptible	PT54
MET S1-003	C1	Virchow	Food	Susceptible	NA
MET S1-011	B	Agona	Food	KSTSfN	NA
MET S1-220	D	Typhi	Human	Sf	PT23
MET S1-184	B	Paratyphi B	Human	Susceptible	PT15

*Bold samples were used for phage isolation. **Antimicrobial resistance profiles of the isolates were determined according to the Clinical Laboratory Standards Institute's (CLSI) standards (CLSI 2013) in our previous study (Acar et al. 2017). Ak: amikacin, Amc: amoxicillin-clavulanic acid, Amp: ampicillin, C: chloramphenicol, Cip: ciprofloxacin, Cn: gentamicin, Cro: ceftriaxone, Eft: ceftiofur, Etp: ertapenem, Fox: ceftiofur, Ipm: imipenem, K: kanamycin, Kf: cephalothin, N: nalidixic acid, S: streptomycin, Sf: sulfisoxazole, Sxt: sulfamethoxazole-trimethoprim, and T: tetracycline. The susceptibility limits of antimicrobial agents except ceftiofur were determined by the CLSI's latest report (CLSI 2013).*** XbaI PFGE was performed according to the Centers for Disease Control and Prevention PulseNet protocol (Ribot et al. 2006) in our previous study (Acar et al. 2017).

Morphological classification by high-contrast transmission electron microscopy

To categorize phage morphotypes based on their physical structures and shapes, 10 bacteriophages were analyzed using high-contrast transmission electron microscopy (CTEM) (Ackermann 2009). A fresh phage stock (1 ml) with a high titer was centrifuged at 21 000 × g for 90 min. The supernatant was discarded, and 1 ml of 0.1 M ammonium acetate solution was added. A volume of 10 ml of the solution were dropped onto the TEM grid and left for 2 min. The droplet was collected using filter paper, and 10 ml dye was promptly added. Sodium phosphotungstate (2%, pH 7.2) was used as dye. After 2 min, the remainder was removed using fil-

ter paper. The grids were left to dry for 10 min and were sent to the METU Central Laboratory. Images were processed using ImageJ software. After phage morphology was determined, phages were given unique identifiers containing information about phage morphology and host (Adriaenssens and Rodney Brister 2017)

One-step growth curve, latent period, and burst size

One-step growth curve experiments were performed using the method described by Clokie and Kropinski, with minor modifications (Clokie and Kropinski 2009). At multiplicity of infection (MOI) of 0.01, 0.1 ml phage suspension (10⁶ PFU/ml) was added

to 9.9 ml *Salmonella* host culture (10^8 CFU/ml) and incubated for 5 min at 37°C, allowing bacteria to absorb phages. After incubation, 0.1 ml of the phage–host mixture was transferred to pre-warmed 9.9 ml LB broth and from there 1 ml was transferred to 9 ml LB broth. A volume of 0.1 ml was removed from all phage–host dilutions, and a double plaque assay was performed at 6 min intervals for 90 min. The plates were incubated at 37°C for 24 h to determine phage titers. The latent period and burst sizes of the phages were calculated according to one-step growth curves.

Adsorption curve

The adsorption curves were determined as described by Clokie and Kropinski (2009). The target strains were incubated overnight in brain–heart infusion broth at 37°C. The titers of the phages used in this experiment were adjusted to 10^6 . A volume of 950 µl LB broth was added to 12 Eppendorf tubes, which were placed on ice and allowed to chill before the experiment. A volume of 9 ml of the mid-exponential phase culture were added to the beaker. A volume of 1 ml of the phage suspension was added to the beaker, and the timer was started. At 1-min intervals for 10 min, 0.05 ml sample was taken from the beaker and added to a chilled Eppendorf tube. Then, by taking a 100 µl sample from the chilled Eppendorf to soft LB and adding the target strain, the double plaque assay was performed. All plates were incubated overnight at 37°C. The next day, plaques were counted, and following formula was used to determine the adsorption rate constant, k (ml/min), where B is the concentration of bacterial cells (CFU/ml), and t is the time interval (seconds) in which the titer decreased from P_0 (initial PFU/ml) to P (final PFU/ml).

$$k = \frac{2.3}{Bt} \log \frac{P_0}{P}$$

Phage genome size determination

The PFGE protocol suggested by Lingohr et al. (2009) was followed for genome size determination of the isolated bacteriophages. Freshly prepared bacteriophages with high titers ($>10^8$ PFU/ml) were collected using SM buffer First, 400 µl of molten 1.2% agarose was mixed with 400 µl of the phage suspension and plugs were prepared. After solidification, the plugs were transferred to tubes containing 5 µl phage lysis buffer [50 mM Tris, 50 mM EDTA, and 1% (w/v) SDS] and 25 µl Proteinase K (20 mg/ml) solution. Plugs were incubated for 2 h at 54°C with shaking, washed twice with sterile deionized water at 54°C, and four times with Tris-EDTA Buffer (10 mM Tris, 1 mM EDTA) at 54°C. Each plug was sliced to 2 mm and loaded into preprepared PFGE agarose (1% SeaKem Gold Agarose; $0.5 \times$ TBE). The gel was placed in a PFGE chamber. A volume of 836 µl of thiourea solution (10 mg/ml) was added to the buffer immediately before use. Migration was performed using a CHEF-DR III System (Bio-Rad) for 19 h at 14°C with electric field of 6.0 V.cm⁻¹ and an angle of 120°. After the run, the gel was stained with 10 mg/ml ethidium bromide solution and destained sterile deionized water. *Salmonella* Braenderup (MET S1-713) was used as reference.

Bacteriophage DNA extraction, genome sequencing, and analysis

DNA purification of phages was done by using Norgen Biotek Phage DNA isolation kit (Thorold, Canada) according to the manufacturer's protocol. DNA sequencing of phages was performed by Illumina NovaSeq platform commercially (BM Lab, Ankara).

Bioinformatic analysis of DNA sequences was performed using the methods and software reported by Shen and Millard (2021). Quality control was performed using FASTQC (<http://www.bioinformatics.babraham.ac.uk/projects/fastqc/>), and Bbduk (<https://sourceforge.net/projects/bbmap>) was used to trim the raw reads. SPAdes version 3.9.0 (Bankevich et al. 2012) was used to assemble the phage genome. The quality of the assemblies was assessed using QUAST (Gurevich et al. 2013). Bandage was used to visualize the assemblies (Wick et al. 2015). The constructed genomes were first checked for their nearest relatives using BLASTn against the Caudovirales database. Prokka was used for structural and functional annotation (Seemann 2014). Multiple phage genome alignments were performed using Clinker (Gilchrist and Chooi 2021). Taxonomic characteristics such as family and subfamily were identified by using NCBI taxonomy chart. To screen for virulence, antibiotic resistance and temperate lifecycle genes, VFDB, ResFinder 4.1 and PhageLeads were used respectively (Liu et al. 2019, Bortolaia et al. 2020, Yukgehnaish et al. 2022). Additionally, in order to observe variety among phage-encoded enzymes, multiple alignments were performed using MEGA 11, and phylogenetic trees were generated (Tamura et al. 2021). Interpro was used to identify the protein families of phage-derived proteins (Paysan-Lafosse et al. 2023). I-tasser was utilized to predict the ligand-binding sites (LBSs) and structure of phage-derived proteins (Zhou et al. 2022).

Bacterial reduction and virulence index

Effectiveness of phages against target bacteria was characterized by planktonic killing assay and virulence index (Storms et al. 2020). Mid-log culture of host was adjusted to 10^8 CFU/ml by using spectrophotometer (OD₆₀₀ = 0.1). Also, fresh phage titers were prepared, and titers were adjusted to 1×10^9 PFU/ml. 96-well plate was used for this analysis. In the first four wells of first column 180 µl phage free bacteria added as control and in the last four columns, 180 µl LB broth with colistin (512 mg/l) were added as blank. A volume of 180 µl bacteria was added to rest of the wells. Phage stocks were diluted from 10^8 to 10^1 PFU/ml, so that MOI of the wells ranged from 1 to 10^{-7} . Phage samples were experimented in triplicate using the MULTISKAN SKY plate reader at a 37°C incubation temperature. The OD (600 nm) was measured every 5 min for 24 h, with the plate shaken for 5 s before each reading. Virulence index was calculated from the area difference between the control (phage free bacteria) and each reduction curves by using the following formula where V_i is the virulence index, A_i is the area of phage killing curve, and A_0 is the area of bacterial growth curve. Areas were calculated according to trapezoid rule. This experiment was conducted in triplicate, and the standard deviations were computed accordingly.

$$v_i = 1 - \frac{A_i}{A_0}$$

Statistical analysis

Statistical analyses were performed using RStudio (Integrated Development for R. RStudio, PBC, Boston, MA). Poisson regression and logistic regression was performed to show that bacteriophages isolated from wastewater had a wider host range than those isolated from farms. A mixed-effects logistic regression was performed to examine the seasonal variation in the prevalence phages. The one-way ANOVA conducted on the virulence index data of the different phages at varying concentrations of PFU/ml.

Differences were considered statistically significant when P-value was less than .05.

Results and discussion

Bacteriophage isolation and purification

In this study, 97 phages with different morphology out of 90 samples were isolated, purified, and stored at 4°C and -80°C. Of these, the highest number of phage ($n = 41$) was achieved using *S. Enteritidis* as a host, followed by *S. Typhimurium* ($n = 28$), *S. Infantis* ($n = 12$), *S. Kentucky* ($n = 5$), *S. Hadar* ($n = 4$), *S. Anatum* and *S. Telaviv* ($n = 3$) each, and *S. Montevideo* ($n = 1$) hosts. Detailed information is provided in [Supplementary Table 2](#).

Since for phage isolation in all samples, *S. Enteritidis*, *Typhimurium*, and *Infantis* isolates were employed, the prevalence of phages isolated by utilizing these hosts was compared both temporally (cattle and poultry farms, and wastewater facilities) and spatially (spring, summer, fall, and winter). In that case, the overall *Enteritidis* phage isolation rate was the highest (46%, 41/90), and similarly, among three different locations (cattle farm, poultry farm, and wastewater facilities) the isolation rate from the poultry farms was the highest (62%, 23/37). This trend was observed for *Typhimurium* phages, because *Enteritidis* phages coinfect *Typhimurium* isolates. In addition, the prevalence of *Enteritidis* phages showed a notable seasonal trend. The number of phages isolated during the summer increased from 12 to 23 during the winter months. A mixed-effects logistic regression was performed to examine the seasonal variation in the prevalence of *Enteritidis* phage. It was found that the prevalence significantly increased during the fall ($P = .015$) and winter ($P = .008$) compared to the summer, whereas no significant difference was observed in the spring. However, these differences might also be attributed to potential unidentified sampling biases, such as variations in sampling locations. Further research is therefore required to test this hypothesis (Table 2).

Interestingly, the overall isolation rate, as well as the isolation rate in poultry farms of *Infantis* infecting phages was the lowest; 13% and 9%, respectively. This was particularly unexpected, since the prevalence of *S. Infantis* isolates has been reported to be the highest for *Salmonella* serotypes in poultry farms in Türkiye (Durul et al. 2015, Gıda ve Kontrol Genel Müdürlüğü 2018). This situation can be explained by the fact that the isolates *S. Infantis* may have acquired resistance to phages.

All phages in this study had titers above 10^8 CFU/ml after isolation. We observed that the phages isolated using *S. Enteritidis* and *S. Typhimurium* as hosts reached higher titers than the other phages. Thus, it is possible to state that they are more prevalent and/or replicate more quickly inside the bacterial populations. Therefore, they may be more potent in managing or eliminating bacterial populations.

Host-range determination

The lytic profiles of the bacteriophages on different hosts were evaluated to determine their host ranges. The efficacy of 97 isolated bacteriophages was tested on 36 *Salmonella* isolates, representing 18 different serovars (Table 1). Overall, 23 phages lysed 20 (20/36) or more host cells ([Supplementary Table 3](#)). Thus, they are termed as broad host range infecting phages. The broadest host range was detected for MET P1-091, which was isolated from chicken manure using *S. Infantis* as a host. This phage completely and partially lysed 28 *Salmonella* isolates (28/36). In this study, we could not isolate any phages fully infecting *S. Mbandaka*, which is

a rare serotype in Türkiye. Furthermore, phages isolated by using *S. Enteritidis* (MET S1-001) as a host, also infected *S. Enteritidis* isolates in our host range isolate list (Table 1), this trend is also observed for *Typhimurium* phages. However, phages, isolated by using *S. Infantis* as a host cannot infect all *Infantis* isolates in our host range isolate list. In addition, the efficacy of phages was analyzed for *S. Typhi* and *S. Paratyphi*, which are typhoidal serovars. The results showed that among 97 phages, *S. Typhi* was infected by only six different phages, whereas *S. Paratyphi B* was lysed by the 89 isolated phages.

The results of this study suggest that bacteriophages isolated from wastewater were more diverse and have broader host ranges than those isolated from farms. To prove this statistically, Poisson regression and logistic regression was performed, and it was seen that phages isolated from wastewater were found to have a significantly different host range than those isolated from farms ($P < .05$). Akhtar et al. (2014) also reported a similar conclusion that it is more likely to isolate phages with broad host ranges from wastewater than manure. This trend might be due to the fact that phages in wastewater encounter a higher diversity of hosts, as wastewater includes various sources, such as animal, human, and environmental wastes. In addition, Parmar et al. (2018) stated that a diverse bacterial community drives the diverse bacteriophage prevalence due to the frequent changes in bacterial populations.

As a result of host range determination, 10 phages (MET-P1-001, MET-P1-082, MET-P1-091, MET-P1-100, MET-P1-103, MET-P1-116, MET-P1-122, MET-P1-137, MET-P1-164, and MET-P1-179) with the broadest host range and infecting the most common serotypes were selected and used for further analysis (Table 3).

Morphological classification by CTEM

CTEM images were used to determine the morphology of the 10 phages. Head and tail measurements were performed by processing the remaining images using ImageJ software (Table 4). Three *Enteritidis* phages (MET P1-001, MET P1-082, and MET P1-103), originally isolated from *Enteritidis* hosts, had distinguishable base plates and shorter tails; therefore, they were named *Myoviridae*, vB_SenM-001, vB_SenM-082, and vB_SenM-103, respectively. While the other two phages originally isolated from *Enteritidis* host (MET P1-122 and MET P1-164), had isometric capsids and longer tails with an attached baseplate, they were named as *Siphoviridae*, vB_SenS-122, vB_SenS-164, respectively. Rest of the phages also showed characteristics of the *Siphoviridae* morphotype. Morphological classification by using CTEM was widely used and gave more common ground information that can be interpreted by researchers in this field. *Caudoviridae* was divided into three families, *Myoviridae*, *Siphoviridae*, and *Podoviridae* (Ackermann 2007) and this classification was generally used for phages previously. However, with technological improvements, classification of phages based on morphology was shifted to a genome-based taxonomy by the International Committee on Taxonomy of Viruses, therefore order *Caudovirales* and families *Myoviridae*, *Podoviridae*, and *Siphoviridae*, determined by CTEM, were abolished (Turner et al. 2023). Therefore, these phages were also sequenced for taxonomic classification.

One-step growth curve, latent period, and burst size

One-step growth curve is performed to measure the latent period (the time required for a bacteriophage to initiate and complete its reproductive cycle), and the burst size (the number of phages released per infected host) of phages. While burst size and latent

Table 2. Number of isolated phages with respect to seasons.

	Number of sample	Isolated Enteritidis phage	Isolated Infantis phage
Summer	24	12	1
Winter	23	23	1
Fall	22	16	9
Spring	21	17	1

Table 3. Host range of 10 selected phages.

Serotype	METUID	P1-001	P1-082	P1-103	P1-122	P1-164	P1-091	P1-100	P1-116	P1-179	P1-137
S. Enteritidis	MET S1-742	+	+	+	+	+	T	T	T	+	T
S. Enteritidis	MET S1-217	-	+	P	-	-	T	+	+	+	+
S. Enteritidis	MET S1-221	+	+	T	+	T	T	-	-	T	T
S. Enteritidis	MET S1-411	+	+	+	+	+	T	-	T	+	T
S. Enteritidis	MET A2-012	+	+	+	+	T	-	-	-	P	-
S. Typhimurium	MET S1-223	+	+	T	T	T	T	-	-	T	-
S. Typhimurium	MET S1-185	T	T	+	+	+	T	-	-	+	-
S. Typhimurium	MET S1-663	T	+	+	T	+	T	-	-	-	-
S. Typhimurium	MET A2-003	T	+	+	+	T	T	-	-	T	-
S. Typhimurim	MET A2-088	+	+	+	+	+	T	+	+	T	+
S. Typhimurium	MET S1-657	+	+	T	T	+	T	-	-	T	-
S. Infantis	MET S1-050	-	-	T	+	+	+	+	+	-	T
S. Infantis	MET S1-807	-	-	P	T	-	+	+	+	-	-
S. Infantis	MET S1-857	T	-	-	-	-	+	+	+	T	T
S. Kentucky	MET S1-240	-	-	-	T	-	+	+	+	-	+
S. Kentucky	MET S1-542	T	T	+	T	T	+	+	+	T	+
S. Kentucky	MET A2-072	-	T	-	-	-	+	T	T	-	+
S. Montevideo	MET S1-065	-	-	T	T	T	T	+	T	T	-
S. Montevideo	MET S1-170	T	-	T	T	T	T	T	T	T	-
S. Montevideo	MET S1-172	-	-	-	-	T	-	T	T	T	T
S. Anatum	MET S1-548	T	T	+	+	-	+	+	+	T	T
S. Anatum	MET S1-579	T	-	-	-	T	-	-	-	-	-
S. Hadar	MET S1-163	-	-	-	-	-	-	-	-	-	T
S. Telaviv	MET S1-074	+	-	+	+	+	+	+	+	+	T
S. Telaviv	MET S1-530	-	-	T	T	T	+	T	T	-	T
S. Thompson	MET S1-008	-	T	T	-	-	T	+	+	-	-
S. Senftenberg	MET S1-010	+	+	-	-	-	-	-	-	-	-
S. Othmarschen	MET S1-087	-	-	T	T	-	T	T	+	T	-
S. Newport	MET S1-166	-	-	-	-	-	+	-	-	+	T
S. Braenderup	MET S1-713	-	-	-	-	-	T	+	+	-	-
S. Mbandaka	MET S1-864	-	-	-	-	-	-	-	-	T	-
S. Liverpool	MET A2-099	-	-	-	-	-	-	-	-	-	-
S. Virchow	MET S1-003	+	+	+	-	T	-	T	T	T	+
S. Agona	MET S1-011	-	+	+	T	-	+	+	T	-	-
S. Typhi	MET S1-220	-	-	-	P	T	-	+	+	T	T
S. Paratyphi B	MET S1-184	+	T	+	T	+	T	+	T	T	T

*: +: complete clearing, T: substantial turbidities throughout the cleared zone, P: a few individual plaques, and -: no clearing.

period alone do not directly imply that the phage can be used as a biocontrol agent, they are essential characteristics for phages to be used in applications, particularly when combined with other characteristics. A total of 10 bacteriophages and their target serovars were used to construct growth curves, and their latent periods and burst sizes were determined (Supplementary Fig. 1 and Table 5). The highest burst size of the phages was observed for MET P1-001 (120 PFU/cell), and the shortest latent period (30 min) was observed for MET P1-103, MET P1-122, and MET P1-164. These five phages were originally isolated by using *S. Enteritidis* isolate (MET S1-001). The average latent period of phages isolated by *S. Enteritidis* host was found to be 32.4 min, which is shorter than that of other phages. Similarly, the average burst sizes of *S. Enteritidis* phages were calculated to be 62.4 PFU/cell (Table 5). For the rest of the phages, the latent periods were longer, and burst

sizes were found to be much smaller. For example, the latent periods of phages originally isolated by using *S. Infantis* isolate were found to be 63 min on average and the average burst sizes of these phages were calculated to be 21.3 PFU/cell. Therefore, it can be concluded that phages targeting *S. Enteritidis* had a larger burst size with a shorter latent period. Overall, we observed that the burst size of phages might be affected by bacterial serotypes. This finding was also in a line with a study conducted by Petsong et al. (2019). However, the relationship between burst size and the latent period is not always correlated (Prathibha and Ranasinghe 2019). For instance, although Park et al. (2012) related the shorter latent period to larger burst sizes, Wang (2006) stated that longer latent periods can result in larger burst sizes. In this study, we observed that longer latent periods might lead to smaller burst sizes; however, this may not be accurate for the opposite.

Table 4. Morphological feature of the phages.

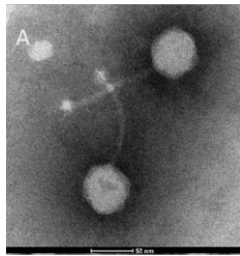
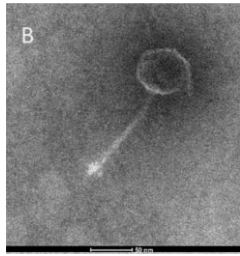
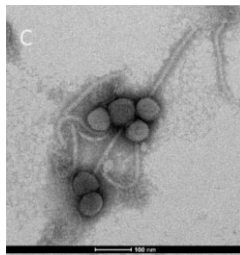
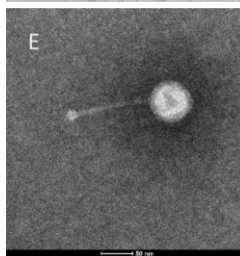
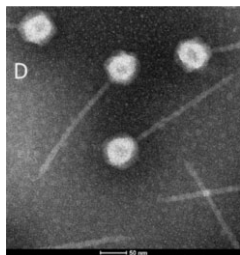
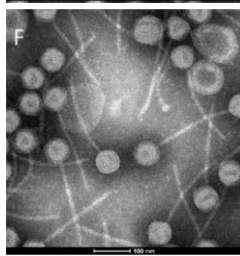
METU-ID	Phage name	Head (capsid) size (nm)	Tail size (nm)	CTEM analysis
MET-P1-001	vB_SenM-001	62.05 ± 4.5	116.53 ± 9.9	
MET-P1-082	vB_SenM-082	98.54 ± 14.9	153.16 ± 5.5	
MET-P1-091	vB_SenS-091	72.38 ± 6.7	200.12 ± 20.5	
MET-P1-103	vB_SenM-103	54.62 ± 6.2	103.05 ± 4.7	
MET-P1-100	vB_SenS-100	50.64 ± 3.4	201.63 ± 4.9	
MET-P1-116	vB_SenS-116	79.86 ± 2.4	221.07 ± 9.6	

Table 4. Continued

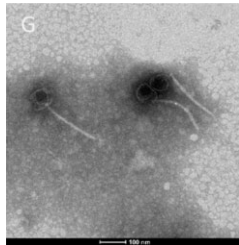
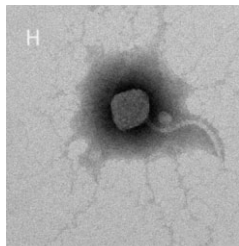
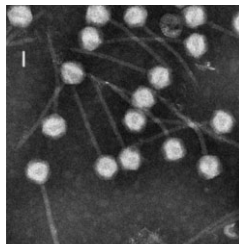
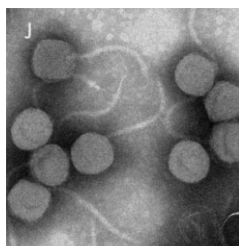
METU-ID	Phage name	Head (capsid) size (nm)	Tail size (nm)	CTEM analysis
MET-P1-122	vB_SenS-122	70.21 ± 13.0	199.76 ± 8.8	
MET-P1-137	vB_SenS-137	67.70 ± 3.7	160.96 ± 4.8	
MET-P1-164	vB_SenS-164	60.76 ± 6.6	220.66 ± 17.5	
MET-P1-179	vB_SenS-179	69.13 ± 3.8	165.66 ± 28.2	

Table 5. Burst size, latent period, and adsorption constants of the bacteriophages.

Phage ID	Host	Latent period (min)	Burst size (PFU/cell)	Free phage (%)*	Adsorption constant (k)
MET P1-001	Enteritidis	36	120	4.2	8.46E-07
MET P1-082	Enteritidis	36	39	6.4	8.04E-06
MET P1-103	Enteritidis	30	64	6.9	7.96E-06
MET P1-122	Enteritidis	30	35	6.7	7.90E-07
MET P1-164	Enteritidis	30	68	13.2	7.30E-07
MET P1-091	Infantis	60	18	12	7.42E-07
MET P1-100	Infantis	60	30	8.7	7.73E-07
MET P1-116	Infantis	72	21	6.2	8.07E-07
MET P1-179	Infantis	60	16	11.1	7.5E-07
MET P1-137	Kentucky	66	18	9.6	7.63E-07

*Free phage % at the end of 10 min.

For biocontrol applications, one of the desired properties is larger burst sizes with shorter latent periods, because they are the indicators of rapid replication and effective phage release (Park et al. 2012, Li et al. 2021). Thus, the phages (MET P1-001, MET P1-103,

and MET P1-164), originally isolated with Enteritidis in our study, which had latent periods from 30 to 36 min with 64–120 PFU/cell burst sizes, might be the most favorable for biocontrol applications in our study.

Adsorption curve

The adsorption curve was used to analyze the rate and effectiveness of phage attachment to host cells. Among 10 phages investigated in our research, MET P1-001 displayed the best adsorption rate (4.2% free phage in 10 min) (Supplementary Fig. 2 and Table 5). In contrast, Infantis and Kentucky phages showed the slowest adsorption results. The results showed that phages originally isolated by Infantis isolates varied in adsorption curves, similar to burst sizes and latent periods. For example, MET P1-179, originally isolated using Infantis, shares similar characteristics with MET P1-137, originally isolated using the Kentucky host. Since we used the original hosts for determination of adsorption curves for 10 phages, these values might vary for different hosts that they can infect.

Phage genome analysis

A total of 10 phages with the widest host-range including the most common serotypes causing diseases were whole genome sequenced by Illumina platform. The raw reads were processed according to the workflow described by Shen and Millard (2021). Among 10 assemblies, in eight of them, multiple phage genomes were detected with acceptable coverages (25X-200X). A total of six assemblies (MET P1-001, MET P1-122, MET P1-164, MET P1-091, MET P1-100, and MET P1-116) exhibited the presence of two phage genomes, whereas in two assemblies (MET P1-082 and MET P1-103) displayed the presence of three phage genomes. In only two assemblies (MET P1-137 and MET P1-179) there was only one phage genome. Presence of multiple phage genomes were re-evaluated in detail. Different-shaped plaque morphologies were not observed for those phages, and phenotypic features such as one-step and adsorption did not indicate the presence of two or more viruses. This situation can be explained by coinfection phenomenon (Díaz-Muñoz 2017), in which coinfection is the simultaneous infection of two phages to same host and is common in nature. These phages could be either lysogenic or lytic. When two phages coinfect the same host, they compete for the host resources (Chevallereau et al. 2022). In this case, only the dominant phage morphology could be observed. For example, the phage MET P1-103 has three phage genomes however, three different plaque morphologies were not seen in phenotypic tests (Table 6).

In our study, we observed seven unique phage genomes obtained from 10 phage samples, and all these unique phages were deposited in the NCBI database (Table 6). For convenience, phages were renamed based on their genome sizes. One of the phage sequences (MET P1-103) showed prophage contamination and was obtained in a single contig and characterized (MET_P1_103_31). The assembled genomes were initially checked using BLAST to identify close relatives (Supplementary Table 4). Phage annotations were made using closely related and well-defined phage genomes. Annotation results revealed that the phage genomes were highly packed with coding sequences (CDS). This phenomenon has been observed in many phage genomes in literature, where phage genomes have very short gaps and even small overlaps between genes (Turner et al. 2021).

The genome-based taxonomy of phages in this study was determined using the BLAST Taxonomy Browser (Table 6). All sequenced phages were identified within the Heunggongvirae kingdom, Uroviricota phylum, and Caudoviricetes class. Depending on the host isolates, phages were varied, except phage with approximately 58 kb size, related to phage Chi, belonging to the *Casjensviridae* family, specifically the *Chivirus* genus. Chi like phages (MET_P1_001_58, MET_P1_082_58,

MET_P1_91_58, MET_P1_100_58, MET_P1_103_58, MET_P1_116_58, MET_P1_122_58, and MET_P1_164_58) was detected in all and three phages isolated by Enteritidis and Infantis hosts, respectively. Chi-like viruses, identified in the 60 s, are known to infect various genera, including *Salmonella* (Schade et al. 1967). In contrast to other phages, Chi is a flagellotropic phage, initiating infection by binding to the flagellar filament and utilizing flagella rotation to reach the host cell (Esteves et al. 2021). Interestingly, all the phages isolated with Infantis host in this study included phages belonged to the same family (Demerecviridae), subfamily (Markadamsvirinae) and genus (*Tequintavirus*). In this genus, it was reported that T5-like phages exhibit a *Siphoviridae* morphotype and share characteristics such as number of tRNAs and direct terminal repeats (Wang et al. 2005). Kentucky phage (MET_P1_137_112) shared with the same family and subfamily but represent a different genus (*Eseptimavirus*). Among Enteritidis phages, we observed multiple genuses. The most commonly seen one in Enteritidis phage samples, with approximately 43 kb genome length (MET_P1_001, MET_P1_082, MET_P1_103, MET_P1_122, and MET_P1_164), represent *Jerseyvirus* genus in Guernseyvirinae subfamily. Similarly, in the literature, *Jerseyvirus* has been commonly reported to infect both Enteritidis and Typhimurium (Moreno Switt et al. 2013, Phothaworn et al. 2019, Ge et al. 2022). One of the Enteritidis phage sample (MET P1-082) included a jumbophage (MET P1_082_240) with a genome length of 243 kb. In nature, jumbo phages, ranging from 122 to 316 kb, are relatively rare (Yuan and Gao 2017). MET P1_082_240 jumbo phage belongs to the genus *Seoulviridae*. MET P1_082_240 was genetically close to the jumbophage SPN3US, which was the first *Salmonella* jumbo phage characterized in 2011, and had the same genome length, G + C% content, and two tRNAs (Lee et al. 2011). Lastly, only one prophage (MET_P1_103_31) isolated in Enteritidis isolate, belonging to the *Peduviridae* family and *Peduvirus* genus, was observed, sharing high conservation across different serotypes and geographical regions. This prophage is notably found in Infantis, Typhimurium, and Enteritidis across USA (Tyson et al. 2021). To avoid the confusion, we only uploaded the presented phages to NCBI for accession numbers (Table 6). These representative ones were the unique phages in this study and used for the further bioinformatic analysis.

To further investigate the therapeutic potential of these phages, their genome sequences were screened for antimicrobial resistance, virulence, and temperate lifestyle genes using ResFinder, VFDB, and PhageLeads databases, respectively. None of the phages contained antimicrobial resistance or virulence-associated genes. However, the lysogeny check using PhageLeads revealed the presence of an integrase gene in the chi-like phage (MET P1_122_58 and MET P1_164_58), which was not detected by Prokka. Therefore, it was deemed unsuitable for phage therapy. When the integrase gene was aligned using the BLAST database, a high homology was observed with other chi-like phages. The lysogenic lifestyle of chi-like phages has been reported previously (Phothaworn et al. 2019). Overall, our results indicated that all phages reported in this study were safe for phage therapy, with the exception of chi-like phages (MET P1_122_58 and MET P1_164_58). Further research is required to assess the potential risks associated with using this phage as a biosafety agent.

The identification of unique genomes representing various families, subfamilies, and genera, highlights the complexity of phage communities in nature. These findings broaden our perspective and emphasize the extent of diversity, illustrating the considerable gap that still exists in our knowledge of phage diversity and ecology. In addition, isolating bacteriophages of the same

Table 6. Genomic features of phages.

Phage ID*	Genome size	GC content	Accession number	Family	Subfamily	Genus
MET_P1_001_43	43 282	50	OP389270	Unassigned	Guernseyvirinae	Jerseyvirus
MET_P1_001_58	58 765	56.3	–	Casjensviridae	–	Chivirus
MET_P1_082_43	43 282	50	–	Unassigned	Guernseyvirinae	Jerseyvirus
MET_P1_082_58	58 765	56.3	–	Casjensviridae	–	Chivirus
MET_P1_082_240	243 224	48.4	OQ383623	Unassigned	Unassigned	Seoulvirus
MET_P1_091_58	58 765	56.3	–	Casjensviridae	–	Chivirus
MET_P1_091_107	106 978	39.3	–	Demerecviridae	Markadamsvirinae	Tequintavirus
MET_P1_100_58	58 765	56.3	–	Casjensviridae	–	Chivirus
MET_P1_100_107	106 987	39.3	OQ383620	Demerecviridae	Markadamsvirinae	Tequintavirus
MET_P1_116_58	58 765	56.3	–	Casjensviridae	–	Chivirus
MET_P1_116_107	106 988	39.3	–	Demerecviridae	Markadamsvirinae	Tequintavirus
MET_P1_103_31	31 582	52.1	OQ383618	Peduoviridae	–	Peduovirus
MET_P1_103_43	43 300	50	–	Unassigned	Guernseyvirinae	Jerseyvirus
MET_P1_103_58	58 765	56.3	–	Casjensviridae	–	Chivirus
MET_P1_122_43	43 282	50	–	Unassigned	Guernseyvirinae	Jerseyvirus
MET_P1_122_58	58 765	56.3	OQ383619	Casjensviridae	–	Chivirus
MET_P1_137_112	112 278	39.8	OQ383621	Demerecviridae	Markadamsvirinae	Epseptimavirus
MET_P1_164_43	43 282	50	–	Unassigned	Guernseyvirinae	Jerseyvirus
MET_P1_164_58	58 782	56.3	–	Casjensviridae	–	Chivirus
MET_P1_179_112	112 001	39	OQ383622	Demerecviridae	Markadamsvirinae	Tequintavirus

*Bolded ones are the unique phage genomes found in this study.

genus from different geographies can suggest that phages have been transferred or dispersed across different regions by natural or artificial means, such as wind, water currents, animal vectors, or human activities.

Our findings led to the investigation of varieties in protein sequences of endolysins enzymes that lyse host cells by targeting the PG layer in seven unique phage genomes. To detect the diversity among endolysin amino acid sequences, multiple alignments were made using MEGA 11 and a phylogenetic tree was created (Supplementary Fig. 3). Additionally, protein families were examined using InterPro (Supplementary Table 5).

The interesting finding is that five out of seven unique phage genomes in our study have more than one open reading frames (ORFs) for endolysin (Supplementary Table 5). This trend was seen not in the phages belonged to *Jerseyvirus* (MET_P1_001_43) and *Chivirus* (MET_P1_122_58) genus's. It can be due to the fact that new protein families and domains are continually being discovered. However, in MET_P1_100_107, MET_P1_103_31, MET_P1_137_112, and MET_P1_179_112 multiple endolysin ORFs were encountered. As mentioned before, MET_P1_103_31 is a highly conserved prophage. In MET_P1_103_31, there are two endolysin ORFs; one of these proteins was found to belong to the lysozyme-like domain superfamily and the endolysin lambda-type family, cleaving the (1→4)-beta-glycosidic bond between N-acetylmuramic acid (MurNAc) and N-acetylglucosamine (GlcNAc) residues in bacterial cell wall PG (Bienkowska-Szewczyk and Taylor 1980). However, the other endolysin was found to belong to the Antiholin LysA-like family, known for interacting with holin to prevent cell lysis. It has been determined that members of this protein family are encoded within prophage regions in bacteria (To et al. 2013). Similarly, in MET_P1_100_107, MET_P1_137_112, and MET_P1_179_112, two different endolysin CDS were observed, with one adjacent to the holin gene and the other distant. When the amino acid sequences of these endolysins were aligned to each other, it was seen that the endolysins adjacent to holin (WFG41157.1, WFG41320.1, and WFG41476.1) were similar to each other, and also the endolysins distant from holin were similar to

each other too with high identity (% identity >85%). It has been observed that endolysins adjacent to the holin gene contain the Peptidase M15C domain and belong to the DD-peptidase zinc-binding domain superfamily. The peptidases in the M15, including bacteriophage endolysins, zinc-dependent D-Ala-D-Ala carboxypeptidases and dipeptidases, break short peptide chains in the PG structure (Rawlings and Barrett 1993). It has been observed that endolysins, far from holin (WFG41120.1, WFG41278.1, and WFG41435.1) have the activity of cell wall hydrolase, SleB domain which serves as lytic enzymes responsible for initiating the breakdown of cortex PG, a crucial degradation process for the germination of spores in *Bacillus* species (Li et al. 2012). Further studies should be conducted to identify which endolysins these phages primarily use. Multiple endolysins in different kind of phage genomes have been reported previously. It has been stated that there are two ORFs encoding endolysin in the genomes of *Gordonia* phages GRU1 and GTE5, but since the combined gene products show homology with single proteins in other systems, it has been suggested that they were once encoded by a single gene, and they were accepted as a single product (Petrovski et al. 2012). Based on this hypothesis, when the multiple endolysins in the phages isolated in this study were examined by combining them, it was noticed that they did not show homology with any single system. In another study, two endolysins were found in adjacent genes and close to the holin gene, but it was stated that these endolysins did not show homology as a single product, and this was interpreted as containing two different endolysins with different cleavage sites that act simultaneously. The presence of a dual lytic system containing two holins and two endolysins in *Lactococcus* KSY1 supports this explanation (Chopin et al. 2007). In the contrary, in this study we only observed one holin gene in the genomes that contain two endolysin genes and one of the two endolysins is adjacent to this holin gene.

Different than the other phages, the jumbo phage (MET_P1_082_240) had different endolysin genes, including seven glycosyl hydrolase genes and one lytic transglycosylase gene in its genome, which are not observed in other phages

(Supplementary Table 5). It has been known that jumbo phages, which has glycosyl hydrolase domains in their tail fiber and tail spike proteins, could improve host recognition and infection, even though injecting their large double-stranded genomes poses a greater challenge. The presence of multiple glycosyl hydrolases might explain why the host ranges of jumbo phages are wider, even infecting multiple genera. It was determined that these enzymes are in the immunoglobulin (Ig)-like fold superfamily. The Ig-like fold refers to a protein structural motif that mimics the general shape and arrangement found in Igs (antibodies), providing a common structural foundation for various proteins involved in diverse biological functions including immune response (Halaby and Mornon 1998). Ig-like folds have been detected in phages with tails and double-stranded DNA. In addition, these have been observed in phages that can infect different genera (Fraser et al. 2006). We observed the same trend for this jumbo phage; besides *Salmonella* strains, it can also infect *Escherichia coli* O104: H4 (ATCC:7547) strain. Other group of endolysin found in jumbo phage was the lytic transglycosylase that are known as cell wall glycoside hydrolases, cell wall glycosidases, and PG glycosidases. We observed that this enzyme in the jumbo phage contains transglycosylase SLT domain 1 and belongs to lysozyme-like domain superfamily like the other lytic transglycosylases of jumbo phages in literature (Pei and Grishin 2005, Vermassen et al. 2019).

Although two *Infantis* phages originally (MET P1-100 and MET P1-179) isolated from same strain (MET S1-006, *Salmonella Infantis*) belonged to the same family, subfamily, and genera, and had the similar endolysins (percent identity >97%), they have different host ranges; MET_P1_100_107 phage infected 22 strains while MET_P1_179_112 phage infected 19 strains out of 36 strains in total (Table 3). To compare the genomic diversity of bacteriophages belonging to the same genus, gene clusters were created with Clinker (Fig. 1) and genes with low identities were examined. It was observed that the genes with low identities belonged to tail fiber protein (0.4) and receptor-binding protein (0.3). Tailed phages employ a diverse array of receptor-binding proteins, including tail fibers, tail spikes, and the central tail spike, located at the distal end of their tail, to specifically recognize host receptors. These proteins play an important role in host recognition and infecting the host (Dams et al. 2019); therefore, they might be considered the most critical proteins of bacteriophage infection. It is possible to further differentiate closely related bacteria belonging to the same genus with their tail fiber and receptor-binding proteins. The diversity in these genes indicates differences in host specificity and the potential ability of these phages to infect different bacterial species, as evidenced by host range analysis.

The genes encoding the receptor-binding proteins were further examined using Interpro, but we could not find a specific family. Considering that the structural differences between these proteins may contribute to host range variation, the structures of these proteins were predicted using I-TASSER. According to the I-TASSER results, both MET_P1_100_107 and MET_P1_179_112 phages have a receptor-binding protein structure similar to the T5 phage receptor-binding protein pb5, with a template modeling score of 0.76. Interestingly, the most significant difference was found not in the protein structures but in the LBS. Particularly, intermolecular interactions between proteins and ligands, such as small compounds, occur via amino acid residues at specific positions in the protein, often found in pocket-like regions. These specific key amino acid residues are referred to as LBSs. It was observed that MET_P1_100_107's receptor-binding protein binds to iron-sulfur cluster and 1,2-

dimethoxy-12-methyl[1,3]benzodioxolo[5,6-c]phenanthridin-12-ium, while MET_P1_179_112's receptor-binding protein binds to alpha-D-mannopyranose. Previous studies have emphasized the importance of receptor-binding proteins in terms of host range of bacteriophage (Gencay et al. 2019). Here, we also highlighted significance of LBSs of these proteins for the host range the first time in the literature to our knowledge.

Another gene region with low sequence identity (identity = 40) among these two closely related phages (MET P1-100 and MET P1-179) was identified as a "hypothetical protein" in NCBI. However, these hypothetical proteins from each phage were later analyzed using BLASTP, revealing that the protein of MET_P1_100_107 phage is 79% identical to the tail fiber protein of *Salmonella* phage SE11 (Fong et al. 2019), while the MET_P1_179_112 phage's protein is identical to the tail fiber protein of *Escherichia* phage OSYSP (Yesil et al. 2017). Subsequently, the protein structures were predicted using I-TASSER (Supplementary Fig. 4). Upon examination, both proteins were found to be structurally most similar to RNA-dependent RNA polymerases of transcribing cypoviruses (Hongrong and Lingpeng 2015). Additionally, both of these proteins had the same LBSs, with RNA being the bound ligand.

Bacterial reduction and virulence index

Bacterial reduction was performed to measure phage virulence in liquid media in 96-well plates. Bacterial reduction curves showed the effect of phage titers on bacterial growth. Phages inhibit bacterial growth when the titer was higher than 6 log PFU/ml for at least 4 h (Supplementary Fig. 5). After 4–6 h, host developed resistance, and started to grow in all experiments. Statistical significance of the differences in phage virulence indices at varying PFU/ml concentrations was determined using one-way ANOVA. The analysis included data from three phage groups (*Enteritidis*, *Infantis*, and *Kentucky*), with each group tested at eight different titer concentrations. This analysis supports the statement that *Enteritidis* phages inhibit bacterial growth effectively even at low titers (<5 log CFU/ml), a trend not as strongly observed in the *Infantis* and *Kentucky* phages, with *Infantis* phages notably failing to inhibit bacterial growth at low levels ($P < .05$). When phages were 8 log PFU/ml, bacterial growth was completely inhibited for hours, in all instances (Supplementary Fig. 5). For *Enteritidis* phages, there was no apparent relationship with the host resistance and phage titer. The results showed that there is no linear correlation between the phage titer and host resistance. Host started to grow around same time for all titers. Since *Infantis* and *Kentucky* phages were ineffective at low titers, it might be hosts gained resistance rapidly. Virulence index is the area between host growth curve and host growth curve with phage. Virulence index shows the effectiveness of phage, and it was calculated for all phage titers from 1 log to 8 log PFU/ml (Fig. 2). Expectedly, virulence index was increased with the increased titer in all phages. This analysis helps standardization of phage selection (Haines et al. 2021), however, it should be noted that this analysis is directly related to host. For instance, within our results, we could compare the phages affecting same hosts. Nevertheless, this analysis is particularly useful for cocktail development, as it allows the identification of phage–host combinations (Steffan et al. 2022). In their study, Haines et al. (2021) compared the efficacy of plating and virulence index scores of phages. There was a direct correlation between the methods, and the authors stated that phages with a virulence index score higher than 0.2 could be considered as efficient for a given host. In our analysis, majority of phages had V_i above 0.4 even in low levels.

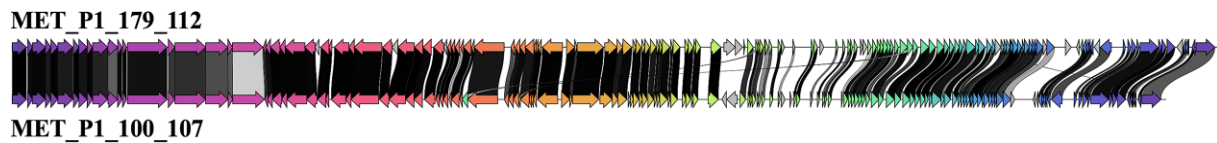


Figure 1. Comparison of genome organization of MET_P1_100_107 and MET_P1_179_112. *Genes are shaded based on sequence identity (0% white, 100% black). The different colors represent clusters of genes that exhibit similarities between two phage genome.

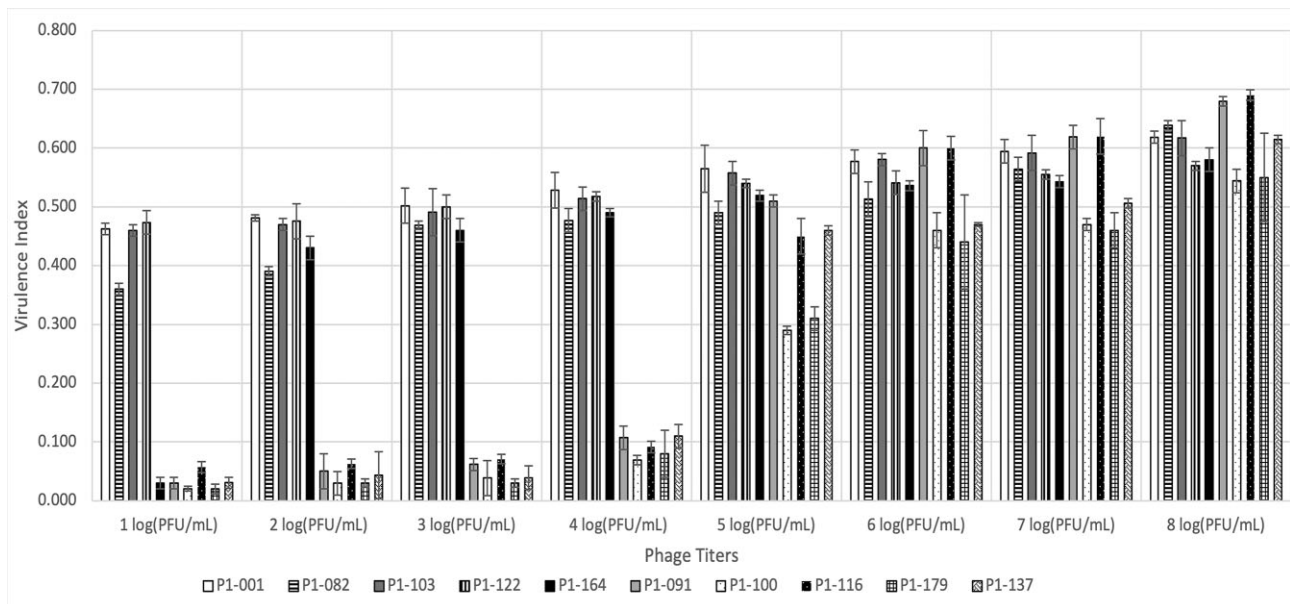


Figure 2. Virulence index of phages. Each experiment was conducted in triplicate, and the standard deviations were computed accordingly.

Conclusion

In conclusion, *Salmonella* is a significant foodborne pathogen that affects millions of people globally each year. Antibiotic resistance of *Salmonella* is a growing public health issue. Alternative approaches, such as phage therapy, to combat the MDR *Salmonella* infections should be further investigated immediately. In this study, 97 different phages were successfully isolated from various sources, highlighting the abundant presence of phages in nature. Furthermore, phages with broad host range were genetically identified, which showed that phages were different genetically, and there was no virulence gene or antibiotic resistance gene in the phage genomes, which demonstrated that they could be used in various applications, except one, which carries lysogenic abilities. Also, endolysin sequence of bacteriophages are investigated and multiple endolysin sequence were observed. Besides, phages isolated from the same host and having the same endolysin sequence but having huge differences in the host range of were observed. Further investigation revealed that LBSs of receptor-binding proteins were the component influencing the host range in this case. Additionally, bacterial reduction curves and virulence indexes proved that these phages are efficient for their host.

In summary, our research has shed light on the rich diversity of bacteriophages in different environments and their potential utility in practical applications. These findings will pave the way for future studies and signify their potential for various applications in fields such as food safety, medicine, and veterinary medicine.

Acknowledgment

We would like to thank Dr. Önay Burak Doğan for his help with the statistical analysis in this study.

Author contributions

Mustafa Guzel (Investigation, Methodology, Writing – original draft), Aysenur Yucefaydali (Formal analysis, Investigation, Methodology, Writing – original draft, Writing – review & editing), Segah Yetiskin (Investigation, Methodology, Writing – original draft), Aysu Deniz (Investigation, Methodology, Writing – original draft), Osman Yaşar Tel (Methodology, Resources, Writing – original draft), Mustafa Akçelik (Methodology, Resources, Writing – original draft), and Yeşim Soyer (Conceptualization, Investigation, Methodology, Project administration, Resources, Visualization, Writing – original draft, Writing – review & editing)

Supplementary data

Supplementary data is available at [FEMSEC Journal](https://academic.oup.com/femsec/article/100/7/fiae079/7685534) online.

Conflict of interest: None declared.

Funding

This study was supported by the Scientific and Technical Research Council of Turkey (TUBITAK) (Project no: 1190345).

References

- Acar S, Bulut E, Durul B et al. Phenotyping and genetic characterization of *Salmonella enterica* isolates from Turkey revealing arise of different features specific to geography. *Int J Food Microbiol* 2017;**241**:98–107. <https://doi.org/10.1016/j.ijfoodmicro.2016.09.031>.
- Ackermann H-W. *Salmonella Phages Examined in the Electron Microscope*. Totowa: Humana Press, 2009.
- Adriaenssens EM, Rodney Brister J. How to name and classify your phage: an informal guide. *Viruses* 2017;**9**:70. <https://doi.org/10.3390/v9040070>.
- Akhtar M, Viazis S, Diez-Gonzalez F. Isolation, identification and characterization of lytic, wide host range bacteriophages from waste effluents against *Salmonella enterica* serovars. *Food Control* 2014;**38**:67–74. <https://doi.org/10.1016/j.foodcont.2013.09.064>.
- Bankevich A, Nurk S, Antipov D et al. SPAdes: a new genome assembly algorithm and its applications to single-cell sequencing. *J Comput Biol* 2012;**19**:455–77. <https://doi.org/10.1089/cmb.2012.0021>.
- Biełkowska-Szewczyk K, Taylor A. Murein transglycosylase from phage X lysate purification and properties. *Biochim Biophys Acta* 1980;**615**:489–96.
- Bortolaia V, Kaas RS, Ruppe E et al. ResFinder 4.0 for predictions of phenotypes from genotypes. *J Antimicrob Chemother* 2020;**75**:3491–500. <https://doi.org/10.1093/jac/dkaa345>.
- Carvalho C, Costa AR, Silva F et al. Bacteriophages and their derivatives for the treatment and control of food-producing animal infections. *Crit Rev Microbiol* 2017;**43**:583–601. <https://doi.org/10.1080/1040841X.2016.1271309>.
- Chevallereau A, Pons BJ, van Houte S et al. Interactions between bacterial and phage communities in natural environments. *Nat Rev Micro* 2022;**20**:49–62. <https://doi.org/10.1038/s41579-021-00602-y>.
- Chopin A, Deveau H, Ehrlich SD et al. KSY1, a lactococcal phage with a T7-like transcription. *Virology* 2007;**365**:1–9. <https://doi.org/10.1016/j.virol.2007.03.044>.
- Clokier MRJ, Kropinski AM (eds.). *Bacteriophages*. Vol. 501. Totowa: Humana Press, 2009. <https://doi.org/10.1007/978-1-60327-164-6>.
- CLSI. *Performance Standards for Antimicrobial Susceptibility Testing; Twenty-Third Informational Supplement*. Vol. 33. Wayne: CLSI, 2013.
- Dams D, Brøndsted L, Drulis-Kawa Z et al. Engineering of receptor-binding proteins in bacteriophages and phage tail-like bacteriocins. *Biochem Soc Trans* 2019;**47**:449–60. <https://doi.org/10.1042/BST20180172>.
- de Kraker MEA, Stewardson AJ, Harbarth S. Will 10 million people die a year due to antimicrobial resistance by 2050?. *PLoS Med* 2016;**13**:e1002184. <https://doi.org/10.1371/journal.pmed.1002184>.
- Díaz-Muñoz SL. Viral coinfection is shaped by host ecology and virus-virus interactions across diverse microbial taxa and environments. *Virus Evol* 2017;**3**. <https://doi.org/10.1093/ve/vex011>.
- Domingo-Calap P, Delgado-Martínez J. Bacteriophages: protagonists of a post-antibiotic era. *Antibiotics* 2018;**7**:66. <https://doi.org/10.3390/antibiotics7030066>.
- Drulis-Kawa Z, Majkowska-Skrobek G, Maciejewska B et al. Learning from bacteriophages—advantages and limitations of phage and phage-encoded protein applications. *Curr Protein Pept Sci* 2012;**13**:699–722.
- Durul B, Acar S, Bulut E et al. Subtyping of *Salmonella* food isolates suggests the geographic clustering of serotype telaviv. *Foodborne Pathog Dis* 2015;**12**:958–65. <https://doi.org/10.1089/fpd.2015.1995>.
- EFSA. The European Union One Health 2021 Zoonoses report. *EFSA J* 2022;**20**. <https://doi.org/10.2903/j.efsa.2022.7666>.
- Esteves NC, Porwollik S, McClelland M et al. The multidrug efflux system AcrABZ-TolC is essential for infection of *Salmonella* Typhimurium by the flagellum-dependent bacteriophage Chi. *J Virol* 2021;**95**:e00394–21. <https://doi.org/10.1128/JVI.00394>.
- Fong K, LaBossiere B, Switt AIM et al. Characterization of four novel bacteriophages isolated from British Columbia for control of nontyphoidal *Salmonella* in vitro and on sprouting alfalfa seeds. *Front Microbiol* 2017;**8**. <https://doi.org/10.3389/fmicb.2017.02193>.
- Fong K, Tremblay DM, Delaquis P et al. Diversity and host specificity revealed by biological characterization and whole genome sequencing of bacteriophages infecting *Salmonella enterica*. *Viruses* 2019;**11**:854. <https://doi.org/10.3390/v11090854>.
- Fraser JS, Yu Z, Maxwell KL et al. Ig-like domains on bacteriophages: a tale of promiscuity and deceit. *J Mol Biol* 2006;**359**:496–507. <https://doi.org/10.1016/j.jmb.2006.03.043>.
- Ge H, Lin C, Xu Y et al. A phage for the controlling of *Salmonella* in poultry and reducing biofilms. *Vet Microbiol* 2022;**269**:109432. <https://doi.org/10.1016/j.vetmic.2022.109432>.
- Gencay YE, Gambino M, Prüssing TF et al. The genera of bacteriophages and their receptors are the major determinants of host range. *Environ Microbiol* 2019;**21**:2095–111. <https://doi.org/10.1111/1462-2920.14597>.
- Gilchrist CLM, Chooi YH. Clinker & clustermap.js: automatic generation of gene cluster comparison figures. *Bioinformatics* 2021;**37**:2473–5. <https://doi.org/10.1093/bioinformatics/btab007>.
- Gurevich A, Saveliev V, Vyahhi N et al. QUASt: quality assessment tool for genome assemblies. *Bioinformatics* 2013;**29**:1072–5. <https://doi.org/10.1093/bioinformatics/btt086>.
- Haines MEK, Hodges FE, Nale JY et al. Analysis of selection methods to develop novel phage therapy cocktails against antimicrobial resistant clinical isolates of bacteria. *Front Microbiol* 2021;**12**. <https://doi.org/10.3389/fmicb.2021.613529>.
- Halaby DM, Mornon JPE. The immunoglobulin superfamily: an insight on its tissular, species, and functional diversity. *J Mol Evol* 1998;**46**:389–400.
- Hongrong L, Lingpeng C. Cryo-EM shows the polymerase structures and a nonspooled genome within a dsRNA virus. *Science* 2015;**349**:1347–50. <https://doi.org/10.1126/science.aaa4938>.
- Huang C, Virk SM, Shi J et al. Isolation, characterization, and application of bacteriophage LPSE1 against *Salmonella enterica* in ready to eat (RTE) foods. *Front Microbiol* 2018;**9**. <https://doi.org/10.3389/fmicb.2018.01046>.
- Lavilla M, Domingo-Calap P, Sevilla-Navarro S et al. Natural killers: opportunities and challenges for the use of bacteriophages in microbial food safety from the one health perspective. *Foods* 2023;**12**:552. <https://doi.org/10.3390/foods12030552>.
- Lee J-H, Shin H, Kim H et al. Complete genome sequence of *Salmonella* bacteriophage SPN3US. *J Virol* 2011;**85**:13470–1. <https://doi.org/10.1128/jvi.06344-11>.
- Li HX, Yang XJ, Zhu XY et al. Isolation and characterization of broad host-range of bacteriophages infecting *Cronobacter sakazakii* and its biocontrol potential in dairy products. *Qual Assur Saf Crops Foods* 2021;**13**:21–44. <https://doi.org/10.15586/QAS.V13I3.890>.
- Li Y, Jin K, Setlow B et al. Crystal structure of the catalytic domain of the *Bacillus cereus* SleB protein, important in cortex peptidoglycan degradation during spore germination. *J Bacteriol* 2012;**194**:4537–45. <https://doi.org/10.1128/JB.00877-12>.
- Lingohr E, Frost S, Johnson Roger P. *Bacteriophages*. Vol. 502. Clokie MRJ, Kropinski AM (eds.), Totowa: Humana Press, 2009. <https://doi.org/10.1007/978-1-60327-565-1>.
- Liu B, Zheng D, Jin Q et al. VFDB 2019: a comparative pathogenomic platform with an interactive web interface. *Nucleic Acids Res* 2019;**47**:D687–92. <https://doi.org/10.1093/nar/gky1080>.

- Matsuzaki S, Rashed M, Uchiyama J et al. Bacteriophage therapy: a revitalized therapy against bacterial infectious diseases. *J Infect Chemother* 2005;**11**:211–9. <https://doi.org/10.1007/s10156-005-0408-9>.
- Moreno Switt AI, Orsi RH, den Bakker HC et al. Genomic characterization provides new insight into Salmonella phage diversity. *BMC Genomics* 2013;**14**. <https://doi.org/10.1186/1471-2164-14-481>.
- Park M, Lee JH, Shin H et al. Characterization and comparative genomic analysis of a novel bacteriophage, SFP10, simultaneously inhibiting both *Salmonella enterica* and *Escherichia coli* O157:H7. *Appl Environ Microb* 2012;**78**:58–69. <https://doi.org/10.1128/AEM.06231-11>.
- Parmar K, Dafale N, Pal R et al. An insight into phage diversity at environmental habitats using comparative metagenomics approach. *Curr Microbiol* 2018;**75**:132–41. <https://doi.org/10.1007/s00284-017-1357-0>.
- Paysan-Lafosse T, Blum M, Chuguransky S et al. InterPro in 2022. *Nucleic Acids Res* 2023;**51**:D418–27. <https://doi.org/10.1093/nar/gkac993>.
- Pei J, Grishin NV. COG3926 and COG5526: a tale of two new lysozyme-like protein families. *Protein Sci* 2005;**14**:2574–81. <https://doi.org/10.1110/ps.051656805>.
- Petrovski S, Tillett D, Seviour RJ. Genome sequences and characterization of the related *Gordonia* phages GTE5 and GRU1 and their use as potential biocontrol agents. *Appl Environ Microb* 2012;**78**:42–7. <https://doi.org/10.1128/AEM.05584-11>.
- Petsong K, Benjakul S, Chaturongakul S et al. Lysis profiles of Salmonella phages on *Salmonella* isolates from various sources and efficiency of a phage cocktail against *S. Enteritidis* and *S. Typhimurium*. *Microorganisms* 2019;**7**:100. <https://doi.org/10.3390/microorganisms7040100>.
- Phothaworn P, Dunne M, Supokaivanich R et al. Characterization of flagellotropic, chi-like *Salmonella* phages isolated from Thai poultry farms. *Viruses* 2019;**11**:520. <https://doi.org/10.3390/v11060520>.
- Prathibha RM, Ranasinghe N. Literature study of virus size, burst size, latent period and genome size across different lytic eukaryotic and prokaryotic virus groups—an overview of traits and possible trade-offs. M.Sc. Thesis, Department of Biology, University of Bergen, 2019.
- Principi N, Silvestri E, Esposito S. Advantages and limitations of bacteriophages for the treatment of bacterial infections. *Front Pharmacol* 2019;**10**. <https://doi.org/10.3389/fphar.2019.00513>.
- Puxty RJ, Millard AD. Functional ecology of bacteriophages in the environment. *Curr Opin Microbiol* 2023;**71**:102245. <https://doi.org/10.1016/j.mib.2022.102245>.
- Rawlings ND, Barrett AJ. Evolutionary families of peptidases. *Biochem J* 1993;**290**:205–18.
- Ribot EM, Fair MA, Gautom R et al. Standardization of pulsed-field gel electrophoresis protocols for the subtyping of *Escherichia coli* O157:H7, *Salmonella*, and *Shigella* for PulseNet. *Foodborne Pathog Dis* 2006;**3**:59–67. <https://doi.org/10.1089/fpd.2006.3.59>.
- Schade SZ, Adler J, Ris H. How bacteriophage λ attacks motile bacteria. *J Virol* 1967;**1**:599–609.
- Seemann T. Prokka: rapid prokaryotic genome annotation. *Bioinformatics* 2014;**30**:2068–9. <https://doi.org/10.1093/bioinformatics/btu153>.
- Shen A, Millard A. Phage genome annotation: where to begin and end. *Phage* 2021;**2**:183–93. <https://doi.org/10.1089/phage.2021.0015>.
- Steffan SM, Shakeri G, Kehrenberg C et al. *Campylobacter* bacteriophage cocktail design based on an advanced selection scheme. *Antibiotics* 2022;**11**:228. <https://doi.org/10.3390/antibiotics11020228>.
- Storms ZJ, Teel MR, Mercurio K et al. The virulence index: a metric for quantitative analysis of phage virulence. *Phage* 2020;**1**:27–36. <https://doi.org/10.1089/phage.2019.0001>.
- Tamura K, Stecher G, Kumar S. MEGA11: molecular evolutionary genetics analysis version 11. *Mol Biol Evol* 2021;**38**:3022–7. <https://doi.org/10.1093/molbev/msab120>.
- To KH, Dewey J, Weaver J et al. Functional analysis of a class I holin, P2 Y. *J Bacteriol* 2013;**195**:1346–55. <https://doi.org/10.1128/JB.01986-12>.
- Turner D, Adriaenssens EM, Tolstoy I et al. Phage annotation guide: guidelines for assembly and high-quality annotation. *Phage* 2021;**2**:170–82. <https://doi.org/10.1089/phage.2021.0013>.
- Turner D, Shkoporov AN, Lood C et al. Abolishment of morphology-based taxa and change to binomial species names: 2022 taxonomy update of the ICTV bacterial viruses subcommittee. *Arch Virol* 2023;**168**. <https://doi.org/10.1007/s00705-022-05694-2>.
- Tyson GH, Li C, Harrison LB et al. A multidrug-resistant *Salmonella infantis* clone is spreading and recombining in the United States. *Microb Drug Resist* 2021;**27**:792–9. <https://doi.org/10.1089/mdr.2020.0389>.
- Gıda ve Kontrol Genel Müdürlüğü. Ulusal *Salmonella* kontrol programı. Ankara: Gıda Tarım ve Hayvancılık Bakanlığı, 2018.
- Velazquez-Meza ME, Galarde-López M, Carrillo-Quiróz B et al. Antimicrobial resistance: one health approach. *Vet World* 2022;**15**:743–9. <https://doi.org/10.14202/vetworld.2022.743-749>.
- Vermassen A, Leroy S, Talon R et al. Cell wall hydrolases in bacteria: insight on the diversity of cell wall amidases, glycosidases and peptidases toward peptidoglycan. *Front Microbiol* 2019;**10**. <https://doi.org/10.3389/fmicb.2019.00331>.
- Vikram A, Woolston J, Sulakvelidze A. Phage biocontrol applications in food production and processing. *Curr Iss Mol Biol* 2021;**40**:267–302. <https://doi.org/10.21775/cimb.040.267>.
- Wang IN. Lysis timing and bacteriophage fitness. *Genetics* 2006;**172**:17–26. <https://doi.org/10.1534/genetics.105.045922>.
- Wang J, Jiang Y, Vincent M et al. Complete genome sequence of bacteriophage T5. *Virology* 2005;**332**:45–65. <https://doi.org/10.1016/j.virol.2004.10.049>.
- WHO. *Salmonella (non-typhoidal)*. Geneva, 2018.
- Wick RR, Schultz MB, Zobel J et al. Bandage: interactive visualization of de novo genome assemblies. *Bioinformatics* 2015;**31**:3350–2. <https://doi.org/10.1093/bioinformatics/btv383>.
- Yesil M, Huang E, Yang X et al. Complete genome sequence of *Escherichia* phage OSYSP. *Genome Announc* 2017;**5**:e00880–17. <https://doi.org/10.1128/genomeA>.
- Yuan Y, Gao M. Jumbo bacteriophages: an overview. *Front Microbiol* 2017;**8**. <https://doi.org/10.3389/fmicb.2017.00403>.
- Yukgehnai K, Rajandas H, Parimannan S et al. PhageLeads: rapid assessment of phage therapeutic suitability using an ensemble machine learning approach. *Viruses* 2022;**14**:342. <https://doi.org/10.3390/v14020342>.
- Zhou X, Zheng W, Li Y et al. I-TASSER-MTD: a deep-learning-based platform for multi-domain protein structure and function prediction. *Nat Protoc* 2022;**17**:2326–53. <https://doi.org/10.1038/s41596-022-00728-0>.